HHS Public Access

Author manuscript

Sci Immunol. Author manuscript; available in PMC 2019 August 17.

Published in final edited form as:

Sci Immunol. 2019 February 22; 4(32): . doi:10.1126/sciimmunol.aav5062.

Optimal therapeutic activity of monoclonal antibodies against chikungunya virus requires Fc-FcγR interaction on monocytes

Julie M. Fox[1], **Vicky Roy**[4], **Bronwyn M. Gunn**[4], **Ling Huang**[5], **Rachel H. Fong**[6], **Melissa A. Edeling**[2], **Matthias Mack**[7], **Daved H. Fremont**[2], **Benjamin J. Doranz**[6], **Syd Johnson**[5], **Galit Alter**[4], **Michael S. Diamond**[1,2,3,#]

[1]Departments of Medicine,Washington University in St. Louis, St. Louis, MO 63110

[2]Pathology and Immunology, Washington University in St. Louis, St. Louis, MO 63110

[3]Molecular Microbiology, Washington University in St. Louis, St. Louis, MO 63110

[4]Ragon Institute of MGH, MIT, and Harvard University, Cambridge, MA 02139

[5]MacroGenics, Rockville, MD 20850

[6]Integral Molecular, Inc., Philadelphia, PA 19104

[7]Regensburg University Medical Center, Regensburg, Germany 93042.

Abstract:

Chikungunya virus (CHIKV) is an emerging mosquito-borne virus that has caused explosive outbreaks worldwide. Although neutralizing monoclonal antibodies (mAbs) against CHIKV inhibit infection in animals, the contribution of Fc effector functions to protection remains unknown. Here, we evaluated the activity of therapeutic mAbs that had or lacked the ability to engage complement and Fc-gamma receptors (FcγR). When administered as post-exposure therapy in mice, the Fc effector functions of mAbs promoted virus clearance from infected cells and reduced joint swelling, results that were corroborated in antibody-treated transgenic animals lacking activating FcγR. The control of CHIKV infection by antibody-FcγR engagement was associated with an accelerated influx of monocytes. A series of immune cell depletions revealed that therapeutic mAbs required monocytes for efficient clearance of CHIKV infection. Overall, our study suggests that in mice, FcγR expression on monocytes is required for optimal therapeutic activity of antibodies against CHIKV, and likely other related viruses.

One Sentence Summary:

[#]**Corresponding author:** Michael S. Diamond, M.D., Ph.D., Washington University School of Medicine, 660 S Euclid Avenue, St Louis, MO 63110. 314-362-2842; mdiamond@wustl.edu.

Authors Contributions: J.M.F., B.M.G, and V.R. performed experiments. J.M.F., B.M.G., G.A., M.S.D. designed the experiments and analyzed the data. L.H., R.H.F., B.J.D., M.A.E., D.H.F., and S.J. contributed key reagents and methodology. J.M.F. and M.S.D wrote the first draft of the manuscript, and all authors provided editorial comments.

Competing interests: M.S.D. is a consultant for Inbios and Sanofi-Pasteur, and is on the Scientific Advisory Board of Moderna. S.J. and L.H. are employees of MacroGenics and have equity. R.H.F. and B.J.D. are employees of Integral Molecular, and B.J.D. is a shareholder of Integral Molecular. The authors have no additional conflicts of interest.

Data and materials availability: Mouse strains and antibodies used are available from the corresponding author upon request.

Anti-chikungunya virus antibodies require FcγR engagement but not complement activation for protection and viral clearance.

Introduction

Chikungunya virus (CHIKV) is a mosquito-transmitted, single-stranded, positive-sense enveloped RNA virus belonging to the Alphavirus genus of the *Togaviridae* family. CHIKV was first isolated from an outbreak in Tanzania in 1952 and historically caused infections in Africa and Asia (1, 2). In 2013, CHIKV emerged in the Caribbean and spread into South and Central America causing over 1.7 million cases including locally acquired infections in Florida (3). While CHIKV is rarely fatal, individuals infected with CHIKV develop fever, rash, myositis, and debilitating polyarthritis that can last for weeks. A subset of infected individuals suffers persistent joint pain and inflammation that endures for months to years (4, 5). Currently, there are no licensed vaccines or therapies to combat the acute or chronic phases of disease.

The CHIKV genome encodes four non-structural proteins (nsP1–4) and five structural proteins (capsid, E3, E2, 6K, and E1) from two open reading frames. During infection, heterodimers of p62 (E3 and E2) and E1 assemble in the endoplasmic reticulum and form trimers. The E3 protein is cleaved by furin in the trans-Golgi compartment, and the E2-E1 heterodimer is transported to the plasma membrane where virion assembly and budding occur (6, 7). The mature virion displays 240 copies of the E2-E1 heterodimer assembled into 80 trimeric spikes (7, 8), which facilitate virus attachment and internalization through its cognate receptor, Mxra8 (9–11).

Multiple animal studies have highlighted the significance of antibodies in protection against CHIKV infection. Passive transfer of CHIKV-immune human γ-globulin protects immunocompromised mice from lethal infection (12). Several candidate vaccines also elicit strongly neutralizing antibody responses (13–16). Mouse and human anti-CHIKV monoclonal antibodies (mAbs) with potent neutralizing activity also have been identified; many inhibit CHIKV infection by blocking fusion or viral egress (17–22). Therapeutic administration of these neutralizing mAbs increased survival in immunocompromised mice and reduced viral burden and disease in immunocompetent mice and non-human primates (17, 23, 24). Although antibodies can limit CHIKV disease, these studies did not address the contribution of antibody effector functions to protection. Since anti-CHIKV mAbs can interact with both free virus and the E2-E1 heterodimer on the cell surface, immune mediated clearance mechanisms, such as antibody dependent cellular cytotoxicity (ADCC), antibody-dependent cellular phagocytosis (ADCP), and complement activation, could contribute to clinical and virological protection.

Here, we evaluated the significance of Fc effector functions for antibody therapeutic efficacy in an immunocompetent mouse model of CHIKV-induced arthritis (25) that more closely approximates human disease compared to a lethal infection model in immunocompromised *Ifnar1*$^{-/-}$ mice (18). Intact versions of anti-CHIKV mAbs were compared to variants lacking appreciable binding to FcγRs and C1q. Fc effector functions were required to reduce foot swelling, accelerate clearance of viral RNA, limit infiltration of immune cells, and reduce

accumulation of proinflammatory chemokines. Fc effector function analysis showed the intact mAbs facilitated phagocytosis of beads coated with CHIKV proteins by mouse monocytes and neutrophils. Cellular depletion studies in mice identified monocytes as a key cell type contributing to mAb-mediated clinical protection and clearance of viral RNA. Overall, these studies indicate that specific Fc effector functions of antibody and engagement of FcγR on monocytes are necessary for developing an optimal therapeutic response against CHIKV infection.

Results

Fc effector functions of mAbs decrease CHIKV disease

We previously showed that combination therapy of two neutralizing anti-CHIKV mAbs (CHK-152 [anti-E2] and CHK-166 [anti-E1]) in the lethal, immunocompromised (*Ifnar1*$^{-/-}$ C57BL/6) mouse model for CHIKV improved survival and reduced resistance compared to single or isotype control mAbs (18, 24). Using this established mAb combination, we assessed protection in an immunocompetent wild-type (WT C57BL/6) murine model of CHIKV-induced musculoskeletal disease where animals develop a biphasic pattern of foot swelling, with separate peaks at 3 and 7 days post-infection (dpi) corresponding to tissue edema and immune cell infiltration, respectively (25, 26). We administered a single injection of the mouse CHK-152 + CHK-166 mAb (both IgG2c subclass) combination (250 μg each; 500 μg total) at 3 dpi, which correlates with the onset of disease signs. MAb treatment reduced the second phase of foot swelling, indicating that CHK-152 and CHK-166 could protect following the onset of disease signs (Fig 1A).

To begin to evaluate the mechanism of antibody protection (*e.g.*, neutralization versus effector function), N297Q recombinant variants of CHK-152 and CHK-166 of a human IgG1 heavy chain subclass were produced; this mutation abolishes an N-linked glycosylation site in the C_H2 domain and creates an aglycosylated antibody that does not interact appreciably with FcγRs or C1q (27). The human IgG1 subclass was chosen because it has similar Fc and complement binding specificities as mouse IgG2c to mouse FcγRs (28). We first confirmed that intact and N297Q variants of CHK-152 and CHK-166 neutralized CHIKV equivalently in cell culture (Fig 1B). Next, *in vivo* studies were performed by administering mAbs at 3 dpi and evaluating foot swelling. Whereas the intact human CHK-152 and CHK-166 mAbs reduced foot swelling markedly on days 6, 7, and 8 post-infection, the N297Q mAb variants diminished swelling only slightly (only at 7 dpi) compared to the isotype control (Fig 1C). To confirm that the differences in foot swelling were not due to disparate levels of intact and N297Q human antibody, we measured concentrations in the foot by ELISA at 5 dpi; similar levels of antibodies were detected (Fig 1D). To determine if both mAbs in the cocktail required effector functions for therapeutic efficacy, mice were treated with either intact or N297Q CHK-152 or CHK-166 at 3 dpi and foot swelling was measured. Whereas the individual intact IgG reduced foot swelling, the N297Q variants did not (Fig 1E–F). These results indicate that effector functions are needed to reduce foot swelling with anti-CHIKV mAb therapy.

To confirm that the requirement of Fc-mediated effector function was not unique to the CHK-152 and CHK-166 combination, we tested IM-CKV063, a neutralizing human mAb

against CHIKV E2 (20, 21), and used different mutations ($L_{234}A$-$L_{235}A$ (LALA)) in the Fc region that abrogate binding to FcγRs and C1q (29). We paired IM-CKV063 with humanized CHK-166, to limit virus escape, and then assessed therapeutic efficacy. Similar to results with CHK-152 and CHK-166, the intact IgG versions of IM-CKV063 and CHK-166 reduced foot swelling at 6 and 7 dpi compared to the isotype control or the LALA/N297Q group (Fig S1A). Administration of intact IM-CKV063 alone at 3 dpi also reduced foot swelling compared to the LALA variant or isotype control (Fig S1B), albeit to a lesser extent than CHK-152 or CHK-166 alone.

Fc effector functions of mAbs reduce CHIKV infection

High titers of CHIKV accumulate in the ipsilateral and contralateral ankles of WT mice by 3 dpi (19), the time of therapeutic mAb administration. We evaluated how the intact and N297Q versions of anti-CHIKV mAbs affected viral clearance, which could impact foot swelling four days later. The ipsilateral and contralateral ankles were harvested 5, 7, or 28 dpi from mice receiving the intact or N297Q combination of humanized CHK-152 + CHK-166 therapy or an isotype control at 3 dpi, and amounts of CHIKV RNA were measured by qRT-PCR. The intact mAbs reduced the levels of CHIKV RNA in the ipsilateral ankle compared to the N297Q mAb-treated or isotype control mAb-treated mice at 5 and 7 dpi but not at 28 dpi, which reflects the persistent phase of infection (30) (Fig 2A). The intact but not N297Q mAbs also reduced the amount of viral RNA in the contralateral ankle compared to the isotype control at both 7 and 28 dpi (Fig S2). Analogously, administration of the intact IM-CKV063 and CHK-166 mAb combination at 3 dpi reduced viral RNA levels at 7 dpi in the ipsilateral ankle compared to the LALA/N297Q or isotype control groups (Fig S1C).

To corroborate these findings, CHIKV RNA was visualized by *in situ* hybridization in the ipsilateral foot 5 or 7 dpi. On 5 dpi, there was intense viral RNA staining in the muscle of the midfoot in mice receiving the N297Q cocktail or the isotype control; animals receiving the intact humanized CHK-152 + CHK-166 mAbs had less staining (Fig 2B). By 7 dpi, CHIKV RNA was faintly detectable in tissue sections from mice treated with the intact mAbs whereas abundant staining was apparent in the N297Q or isotype treated groups (Fig 2B). These results suggest that compared to mAbs lacking Fc effector functions, intact anti-CHIKV mAbs accelerate viral clearance and limit dissemination.

Fc effector function mediated immune cell recruitment during acute CHIKV disease

$CD4^+$ T cells, macrophages, and monocyte recruitment contribute to CHIKV-associated musculoskeletal disease (26, 31, 32). Since the intact anti-CHIKV mAbs reduced the levels of viral RNA (and presumably, viral nucleic acid pathogen associated molecular patterns [PAMPs]), we assessed whether treatment impacted pro-inflammatory cytokine and chemokine expression and immune cell infiltration. CHIKV-infected mice were treated with intact or N297Q humanized mAbs or an isotype control at 3 dpi. After harvesting the ipsilateral ankle at 4 or 7 dpi, pro-inflammatory cytokines and chemokines were analyzed by a Bioplex assay and the cellular infiltrate was analyzed by flow cytometry (Fig S3). At 4 dpi (one day after mAb administration), the ipsilateral feet from mice treated with the intact mAbs had higher levels of proinflammatory cytokines and chemokines (*e.g.*, CCL2, CCL3,

CCL4, CCL5, CCL11, CXCL1, TNF-α, IFN-γ, IL-1α, IL-6, and IL-12 p70) and increased percentages of neutrophils compared to the N297Q mAb or isotype treated groups (Fig 3A–E and Table S1). Treatment with intact mAbs also was associated with greater numbers of $CD45^+$ cells, monocytes, and neutrophils in the foot compared to N297Q mAb or isotype treatment at 4 dpi (Fig 3F). However, the number of MHC class II^+ (activated) monocytes was not different between the groups (Fig 3G).

When pro-inflammatory cytokines and chemokines were analyzed in the ipsilateral feet at 7 dpi, the intact mAb-treated mice showed lower levels of CCL2, CCL3, CCL4, and CCL5 compared to animals treated with N297Q or isotype control mAbs (Fig 3H–K). Other cytokines and chemokines (*e.g.*, CCL11, CXCL1, TNF-α, IFN-γ, IL-1α, IL-6, IL-10, IL-12 p40, and IL-12 p70) were measured, but were not statistically different (Table S1). Cellular analysis of the ipsilateral feet at 7 dpi revealed no significant differences in the frequency of the immune cell populations and a modest reduction in the number of total $CD45^+$ cells, monocytes, monocyte-derived dendritic cells (moDCs), neutrophils, NK cells, $CD4^+$ T cells, $CD8^+$ T cells, B cells, and MHC class II^+ monocytes with intact mAb treatment (Fig 3L–N). Consistent with this observation, pathological analysis of the ipsilateral foot at 7 dpi showed similar immune cell infiltrates in the dorsal midfoot and joint space compared to uninfected mice (Fig S4).

We analyzed the flux of pro-inflammatory cytokines and chemokines or immune cells in greater detail after antibody treatment by comparing their concentrations or cell numbers present at 4 and 7 dpi. For CCL2, CCL3, CCL4, CCL5, and IFN-γ, the intact mAb therapy reduced the levels from 4 to 7 dpi, whereas the N297Q and isotype treated mice maintained or increased these pro-inflammatory molecules (Fig S5). When immune cells were compared between 4 and 7 dpi, all mAb treatment groups showed increased numbers of MHC class II^+ monocytes (Fig 3O). However, the intact mAb-treated mice sustained only a modest increase in $CD45^+$ cells, monocytes, and NK cells compared to N297Q mAb or isotype treated mice (Fig 3P–R). Moreover, the intact mAb-treated CHIKV-infected mice showed reduced numbers of neutrophils at 7 dpi compared to 4 dpi, whereas levels were increased slightly in animals treated with N297Q or isotype control mAbs (Fig 3S). Collectively, these data suggest that virus engagement by intact mAbs promotes accelerated immune cell infiltration at the early phase of swelling (*e.g.*, 4 dpi), but this ultimately results in reduced subsequent cell recruitment into the foot, which correlates with less swelling during the second phase (*e.g.*, 7 dpi).

Clinical and virological protection of anti-CHIKV mAbs is mediated through Fc-FcγR interactions

The N297Q mutation in the human heavy chain abrogates binding to both FcγRs and C1q (27). To determine which of these effector molecules was associated with the clinical and virological phenotypes observed with mAb therapy, we performed analogous treatment studies at 3 dpi with intact humanized CHK-152 + CHK-166 in mice lacking C1q (*$C1q^{-/-}$*) or the Fc receptor common gamma chain (*$FcR\gamma^{-/-}$*), which abrogates expression of all activating mouse FcγRs (FcγRI, FcγRIII, and FcγRIV). The intact CHIKV mAbs still reduced foot swelling in *$C1q^{-/-}$* mice between days 6–8 post-infection (Fig 4A). In

comparison, combination mAb therapy in *FcRγ*$^{-/-}$ mice did not diminish swelling at days 6–7 post-infection, although some effect was observed at 8 dpi (Fig 4B). At 5 dpi, the ipsilateral ankle was analyzed for viral RNA. Anti-CHIKV mAbs did not decrease viral RNA in *FcRγ*$^{-/-}$ mice, whereas levels were reduced (10-fold, $P < 0.0001$) in *C1q*$^{-/-}$ mice (Fig 4C). To verify that this phenotype was not specific to heterologous humanized mAbs in mice, the studies were repeated using the mouse versions of CHK-152 and CHK-166 so the mAbs would be homologous to the host species. Similar to the humanized mAbs, the intact mouse mAbs reduced foot swelling in *C1q*$^{-/-}$ mice but not in *FcRγ*$^{-/-}$ mice at 7 dpi (Fig 4D–E). The intact mouse mAbs also decreased viral RNA in the WT and *C1q*$^{-/-}$ mice but not in the *FcRγ*$^{-/-}$ at 7 dpi (Fig 4F). Additionally, FcγR interactions were necessary to reduce viral RNA levels in other peripheral organs (spleen, Fig 4G). These data suggest that antibody-mediated reductions in foot swelling and viral RNA levels principally are facilitated through activating FcγRs.

We analyzed cellular recruitment into the ipsilateral foot of *FcRγ*$^{-/-}$ or *C1q*$^{-/-}$ mice to determine if the increased cellularity observed in WT mice administered the intact mAbs (Fig 3F) was promoted by activating FcγRs or C1q. CHIKV-infected *FcRγ*$^{-/-}$ or *C1q*$^{-/-}$ mice were treated with intact humanized CHK-152 and CHK-166 or an isotype control mAb at 3 dpi. The ipsilateral foot was collected at 4 dpi and cellular infiltrates were analyzed (Fig S6). In the absence of C1q, treatment with the intact mAbs resulted in increased numbers of CD45^{+} cells, neutrophils, and a trend toward more monocytes compared to the isotype control mAb treated mice (Fig 4H), similar to WT mice (Fig 3E–F). Similarly, in the absence of FcγRs, treatment with intact humanized CHK-152 and CHK-166 also resulted in increased numbers of neutrophils compared to the isotype control (Fig 4I). In contrast, in *FcRγ*$^{-/-}$ mice treated with the intact CHK-152 and CHK-166 mAbs, we observed similar numbers of monocytes or CD45^{+} leukocytes in the ipsilateral foot relative to isotype control mAbs (Fig 4I). Collectively, these data suggest that anti-CHIKV mAb engagement with FcγRs has a dominant effect on monocyte recruitment into the musculoskeletal tissues of the infected foot.

Monocytes are necessary for intact mAbs to reduce CHIKV RNA levels in mice

Fc engagement of FcγRs activates innate immune cells, including NK cells, neutrophils, and monocytes, to clear infected cells through ADCC or ADCP (33, 34). To begin to determine which innate immune cell contributed to the protection observed *in vivo,* analysis of Fc effector functions was performed with beads coated with recombinant CHIKV p62 (E3-E2)-E1 protein, mouse innate immune cells, and murine or humanized intact or N297Q variants of CHK-152 and CHK-166. Compared to the isotype control and N297Q mAbs, the mouse and humanized intact CHK-152 and CHK-166 mAbs facilitated greater phagocytosis of CHIKV antigen-coated beads in primary murine monocytes (Fig 5A–B) and neutrophils (Fig 5C–D). As expected, the murine mAbs were more potent than the human mAbs at promoting phagocytosis in mouse cells. This *ex vivo* data suggest that in mice, monocytes and/or neutrophils may be important for anti-CHIKV mAb effector function.

To determine which cell type was the primary mediator of mAb-dependent clinical protection and viral RNA reduction, using a series of antibodies, we depleted NK cells

(NK1.1$^+$) (Fig S7A–D), monocytes and neutrophils (Ly6G/Ly6C$^+$) (Fig 6A–D), neutrophils alone (Ly6G$^+$) (Fig 6E–H), or monocytes alone (CCR2$^+$) (Fig 6I–L) throughout the course of CHIKV infection. As before, humanized anti-CHIKV mAbs or an isotype control were administered 3 dpi, and tissues were harvested at 7 dpi. Depletion was confirmed in peripheral blood on the day of harvest by flow cytometry (Fig 6A–B, E–F, and I–J, and Fig S7A–B). Of note, when neutrophils were depleted, we observed a mild compensatory increase in circulating monocytes (Fig 6F) and reciprocally, when monocytes were depleted we detected an increase in circulating neutrophils (Fig 6J), which has reported previously in the context of CHIKV infection (35). Despite the large specific reduction in individual cell types, the flow cytometric analysis revealed that for each depletion, a small (0.3 – 2%), residual population was present.

NK cell depletion did not impact foot swelling in the presence of anti-CHIKV mAbs or an isotype control mAb (Fig S7C). As anti-CHIKV mAb therapy still reduced viral RNA levels in the ipsilateral ankle in the absence of NK cells, these cells likely did not mediate clearance of infected cells (Fig S7D). In comparison, depletion of monocytes and neutrophils (Ly6G/Ly6C$^+$ cells) reduced foot swelling starting at 3 dpi compared to the isotype depleted animals (Fig 6C). As this decrease in swelling occurred regardless of administration of anti-CHIKV mAbs, we cannot conclude that monocytes and neutrophils are required for the beneficial clinical effect of mAb therapy. Depletion of monocytes and neutrophils, however, resulted in a significant loss in anti-CHIKV mAb antiviral activity in the ankles of mice (Fig 6D); these data suggest that one or both of these cell types mediates mAb-dependent clearance of CHIKV. In comparison, depletion of neutrophils (Ly6G$^+$ cells) alone did not alter foot swelling following CHIKV infection with or without mAb therapy (Fig 6G) or affect the antiviral activity of anti-CHIKV mAbs in the ankle (Fig 6H). However, in the absence of monocytes alone, anti-CHIKV mAb therapy failed to reduce foot swelling at 7 dpi compared to isotype treated mice (Fig 6K), and the antiviral activity of anti-CHIKV mAbs was lost (Fig 6L). To confirm that the requirement of monocytes was not specific to humanized mAbs in mice, the CCR2 depletion was repeated using the mouse versions of CHK-152 and CHK-166. As observed with the humanized anti-CHIKV mAbs, there was a compensatory increase in neutrophils with monocyte depletion (Fig 6M–N). Consistent with the humanized mAbs results, in the absence of monocytes, the mouse anti-CHIKV mAbs did not reduce foot swelling or viral RNA levels (Fig 6O–P). These results suggest that monocytes are the primary cell type responsible for clinical protection and clearance of CHIKV infection in the affected foot via Fc-FcγR interactions.

Discussion

Although prior studies have established the efficacy of mAb therapy during CHIKV infection, the mechanisms of protection *in vivo* have not been definitively identified. We examined the contribution of Fc effector functions for clinical and virological protection in a murine model of CHIKV-induced arthritis. Using a combination of neutralizing anti-CHIKV mAbs that bind to distinct epitopes of the viral surface glycoproteins, we showed that a functional Fc region is required for optimal protection against foot swelling and CHIKV infection during the acute phase of disease. Consistent with these results, clinical and virological protection with intact mAb therapy was diminished in mice lacking expression of

activating FcγRs. Although intact anti-CHIKV mAb therapy augmented monocyte and neutrophil recruitment and proinflammatory cytokines production during the first phase of disease, these cellular and soluble inflammatory mediators were reduced during the second phase of disease, which correlated with reduced foot swelling at 7 dpi. Cell depletion studies identified monocytes as a key cell type for mAb-dependent reductions in CHIKV RNA and clinical disease in mice.

The significance of antibody Fc effector functions has been described in other viral infections, including human immunodeficiency (HIV), influenza, Ebola, West Nile, and hepatitis B viruses (36–41), although the specific cells mediating this effect *in vivo* is less well characterized. Broadly neutralizing mAbs targeting various epitopes on HIV gp120 clear infected cells through FcγR interactions, and modifications that enhance Fc-FcγR affinity increase antibody efficacy (42). For influenza virus, mAbs targeting the conserved stalk region of the hemagglutinin protect *in vivo,* in part through Fc-FcγR interaction on NK cells and neutrophils (43). We tested combinations of three different anti-CHIKV mAbs targeting spatially distinct epitopes on the virion with a range of neutralization capacity. CHK-152 binds across domains A and B of the E2 protein, CHK-166 binds to domain II of the E1 protein, and IM-CKV063 binds to an intersubunit epitope in domain A of the E2 protein (8, 18, 21). Thus, at least for three distinct epitopes, we observed a requirement of Fc-FcγR interactions for optimal antibody protection following CHIKV challenge. Our data are consistent with a study showing reduced efficacy of the CHK-152 N297Q variant in protecting against foot swelling in mice when administered 18 hpi (18). In a historical study with Semliki Forest virus (SFV), a distantly related alphavirus, cross-reactive anti-Sindbis virus γ-globulin failed to neutralize SFV *in vitro*, but was protective *in vivo,* possibly through ADCC (44). Analogously, prophylaxis with non-neutralizing anti-CHIKV mAbs partially protected *Ifnar1*$^{-/-}$ mice from lethal CHIKV challenge, which suggested a role for Fc effector functions, although this was not directly tested (17).

CHIKV RNA persists for months in musculoskeletal tissues including the joints of infected mice, non-human primates, and humans (45–47). Although administration of the intact mAb combination reduced residual viral RNA levels in the contralateral ankle at day 28 more so than the N297Q variants or isotype control mAbs, in all cases, residual viral RNA still remained. Moreover, no difference in viral RNA clearance among treatment groups was observed in the ipsilateral ankle. The failure to clear viral RNA completely was not due to insufficient levels of antibody, as even weekly 500 μg dosing of anti-CHIKV mAbs did not improve clearance. It is possible that once joint-associated tissues are seeded with CHIKV, complete elimination may be difficult to accomplish with mAb therapy. The basis for clearance failure remains uncertain although CHIKV RNA might be expressed in cells in the joint space that are immune privileged and inaccessible to antibodies or immune cells. Alternatively, the cells that persistently replicate CHIKV RNA may not express sufficient amounts of viral structural proteins on their surface to be targeted by antibody-mediated clearance mechanisms.

Previous studies have shown that monocytes and macrophages can contribute to foot swelling (26, 48). Intact anti-CHIKV mAb therapy at 3 dpi increased infiltration of monocytes and neutrophils one day later, and this was associated with a small but consistent,

concomitant increase in foot swelling. Notwithstanding this occurrence, the increased frequency of the neutrophils associated with intact mAb therapy at 4 dpi ultimately resulted in reduced accumulation of myeloid cells and diminished foot swelling at 7 dpi. Consistent with the temporal changes in recruitment of monocytes and neutrophils, mice treated with the intact mAbs had higher levels of the chemokines CCL2, CCL3, CCL4, and CCL5 at 4 dpi yet reduced levels at 7 dpi compared to the N297Q or isotype control mAbs. Thus, the differences in flux of immune cells in the ankle after intact mAb treatment could explain the improved clinical phenotype. Alternatively, differences in the activation state of infiltrating cells could modulate tissue inflammation and edema. Fc-FcγR but not Fc-C1q interactions were important for the anti-CHIKV mAb-dependent increase in accumulation of $CD45^+$ cells and monocytes. One limitation in explaining these results is that the mechanistic basis for the different phases of swelling and the relationship to viral burden after CHIKV infection still is not fully understood. The impact of Fc-FcγR and C1q interaction on immune cell activation, subset composition, and the tissue microenvironment during CHIKV infection warrants further study to define precisely how antibody therapy modulates joint swelling.

NK cells, neutrophils, and monocytes express activating FcγRs that engage the Fc region of mAbs and induce ADCC and/or antibody-dependent cellular phagocytosis (ADCP) to remove virally infected cells (34). A recent study with influenza A virus used clodronate treatment to identify alveolar macrophages as a key cell type for mAb-mediated viral clearance and survival (43). In our experiments, depletion of NK cells or neutrophils did not change foot swelling or antibody-mediated reduction of CHIKV RNA. However, clearance of CHIKV RNA in mice was compromised by the combined absence of monocytes and neutrophils or depletion of monocytes alone, indicating that the monocytes contribute to clearing viral infection in a mAb-dependent manner. Notwithstanding these results, and independent of anti-CHIKV mAb therapy, depletion of monocytes and neutrophils or monocytes alone but not neutrophils alone resulted in increased viral RNA in the ipsilateral ankle compared to isotype control mAb depleted animals. Previous studies that depleted monocytes with clodronate or using CCR2-DTR^+ mice also observed increased CHIKV burden in the contralateral ankle and serum (26, 32). These data suggest that monocytes are important for controlling CHIKV infection or recruit immune cell subsets that facilitate viral clearance.

In the absence of monocytes alone, anti-CHIKV mAb therapy failed to protect against clinical disease. Indeed, monocyte depletion, regardless of mAb therapy, resulted in increased foot swelling at 7 dpi, and was associated with more circulating neutrophils. Analogously, *Ccr2*$^{-/-}$ mice developed more severe CHIKV-induced disease because of compensatory recruitment of neutrophils and eosinophils (35). Consistent with this idea, when we depleted both monocytes and neutrophils, foot swelling was reduced after CHIKV infection. However, when others have depleted monocytes with clodronate or bindarit, an inhibitor CCL2 production, diminished foot swelling was observed, which suggests that monocyte perturbations at different phases of CHIKV infection may result in distinct clinical disease outcomes (26, 49).

Antibodies can limit CHIKV infection and disease, especially when given prior to or shortly after virus infection (18, 20, 23, 50). Our study identifies specific Fc-FcγR interactions as key determinants of mAb-mediated clearance and clinical protection once infection is established in target tissues. Accordingly, antibody-based therapies against viruses that display structural glycoproteins on the surface of infected cells likely should be optimized for specific Fc effector functions to enhance clearance and minimize disease pathogenesis.

Materials and Methods

Study Design

The goal of this study was to determine if antibody effector functions contributed to protection against infection and clinical disease caused by CHIKV, and arthritogenic alphavirus. Using the mouse model of CHIKV arthritis, we performed passive antibody transfers, qRT-PCR for viral RNA, *in situ* hybridization, flow cytometry, cytokine analysis, *in vitro* functional assays, and *in vivo* antibody-based cellular depletions to evaluate how antibody effector functions modulate infection and disease. The sample size and number of independent experiments are indicated in each of the Figure Legends.

Cells, viruses, and antibodies

Murine mAbs against CHIKV were described previously (18), purified from hybridoma supernatants by sequential Protein A Sepharose and size exclusion chromatography, and buffer-exchanged into PBS. MAbs with human Fc domains were produced recombinantly as previously described (51) in ExpiCHO-S cells at 32°C following the manufacturer's instructions. All mAbs used were tested free of endotoxins using the limulus amebocyte lysate (LAL) test cartridge in the Endosafe Portable Testing System (Charles River). Vero, BHK21, and C6/36 cells were cultured as described (18). The CHIKV La Reunion OPY1 strain was the gift of S. Higgs (Kansas State University) and produced from an infectious cDNA clone (52, 53). Focus reduction neutralization tests (FRNT) were performed as previously described using CHK-11 as the detection antibody (19).

Mouse studies

Experiments were performed in accordance with the recommendations in the Guide for the Care and Use of Laboratory Animals of the National Institutes of Health after approval by the Institutional Animal Care and Use Committee at the Washington University School of Medicine (Assurance Number: A3381–01). All injections with virus were performed under anesthesia with ketamine hydrochloride (80 mg/kg) and xylazine (15 mg/kg).

Four week-old WT C57BL/6J mice were purchased from Jackson Laboratories. Four week-old congenic $C1q^{-/-}$ or FcR common gamma chain deficient ($FcR\gamma^{-/-}$) mice were bred at the Washington University Animal Facility. MAbs CHK-152 mouse IgG2c, CHK-166 mouse IgG2c, WNV E60 (murine isotype control; IgG2c), CHK-152 human IgG1, CHK-166 human IgG1, CHK-152 human IgG1 N297Q, CHK-166 human IgG1 N297Q, IM-CKV063 human IgG1, IM-CKV063 human IgG1 LALA, or WNV hE16 (human isotype control; IgG1) were administered to mice by intraperitoneal injection three days post virus infection. Mice were inoculated subcutaneously in the left footpad with 10^3 FFU of CHIKV

in Hank's Balanced Salt Solution (HBSS) supplemented 1% heat-inactivated (HI)-FBS. Ipsilateral foot swelling was monitored via measurements (width x height) using digital calipers. Mice were sacrificed, perfused with PBS, and tissues were collected 5, 7, or 28 dpi. Tissues were titered by qRT-PCR using RNA isolated from viral stocks as a standard curve to determine FFU equivalents, as previously described (19). Fold change of viral burden was determined by the following calculation using non-log transformed values: mean control titer/ mean experimental titer.

Quantification of human IgG in tissues

Unlabeled goat anti-human kappa antibody that was cross-adsorbed to mouse IgG (Southern Biotech) was bound overnight at 4°C on Maxisorp immunocapture ELISA plates (Thermo Scientific) in a sodium bicarbonate buffer pH 9.3. Wells were washed with PBS + 0.05% Tween 20 (Fisher Scientific) and blocked with blocking buffer (PBS + 2% BSA (Sigma)) for 1 h at 37°C. Ankles were homogenized in DMEM + 2% HI-FBS using a MagNA Lyser instrument (Roche). Ankle homogenates were clarified (12,000 × rpm for 5 min), heat-inactivated at 56°C for 1 h, serially diluted in blocking buffer, and then added to wells for 1 h at 4°C. Plates were rinsed and then incubated for 1 h at 4°C with an HRP conjugated goat anti-human Fc antibody that was cross-adsorbed against multiple animal species (Southern Biotech). Plates were washed and developed with TMB one-step substrate system (Dako). The reaction was stopped with 1 M H_2SO_4, and absorbance was monitored at 450 nm. A standard curve was run in parallel and analyzed using non-linear regression to determine the concentration of the humanized antibodies in tissues.

Histology and viral RNA *in situ* hybridization (ISH)

WT mice were inoculated with 10^3 FFU of CHIKV and treated with indicated anti-CHIKV or isotype control mAbs by intraperitoneal injection at 3 dpi. At 7 dpi, animals were perfused sequentially with PBS and 4% paraformaldehyde (PFA). Ipsilateral feet were collected, and hair was removed using Nair (Church & Dwight). Tissue was fixed for 24 h in 4% PFA, rinsed with PBS and water, and then decalcified for 10 days in 14% EDTA free acid (Sigma) in water at pH 7.2. Decalcified tissue was rinsed, dehydrated, embedded in paraffin, sectioned, and stained with hematoxylin and eosin (H & E).

Viral RNA ISH was performed on tissues from mice at 5 and 7 dpi. Tissue and slides were prepared as described above. ISH was performed using RNAscope 2.5 (Advanced Cell Diagnostics (ACD)) according to the manufacturer's instructions and as previously described using the CHIKV probe (479501) designed and synthesized by ACD (54). Images were acquired on a Nikon Eclipse E400 microscope.

Cytokine and chemokine analysis

Mice were inoculated with 10^3 FFU of CHIKV and treated with indicated anti-CHIKV mAbs or an isotype control by intraperitoneal injection on 3 dpi. Ipsilateral ankles were collected 4 or 7 dpi from PBS-perfused mice. Tissue was homogenized in PBS with 0.1% BSA and analyzed for cytokines and chemokines using a Bio-Plex Pro mouse cytokine 23-Plex (Bio-Rad) following the manufacturer's instructions.

Flow Cytometry

Mice were inoculated with 10^3 FFU of CHIKV and treated with indicated anti-CHIKV mAbs or an isotype control by intraperitoneal injection on 3 dpi. At 4 or 7 dpi mice were perfused with PBS and the ipsilateral feet were disarticulated and the skin was everted. Tissue was digested in RPMI supplemented with 10% HI-FBS, HEPES, collagenase (Sigma) and DNase I (Sigma) for 1 h at 37°C with agitation, strained through a 70-μm filter, and resuspended in RPMI supplemented with 10% HI-FBS. Single cell suspensions were blocked for FcγR binding (BioLegend clone 93; 1:50) and then stained with the following antibodies: CD45 BUV395 (BD Biosciences clone 30-F11; 1:200), CD3 APC-Cy7, PE-Dazzle594, or BV421 (BioLegend clone 145–2C11; 1:100), CD4 FITC (BioLegend clone RM4–5; 1:200), CD8α APC (BioLegend clone 53–6.3; 1:200), NK1.1 PE-Cy7 or PE (BioLegend clone PK136; 1:200), CD11b PerCP-Cy5.5 (BioLegend clone M1/70; 1:200), CD19 BV605 (BioLegend clone 6D5; 1:200), Ly6C Pacific Blue (BioLegend clone HK1.4; 1:200), Ly6G PE-Cy7 (BioLegend clone 1A8; 1:200), CD11c APC (BioLegend clone N418; 1:200), MHC class II (I-A/I-E) A700 or PE (BioLegend clone M5/114.15.2; 1:200), or Ly6B FITC (Abcam clone 7/4; 1:100). Viability was determined through exclusion of a fixable viability dye (e506; eBiosciences; 1:500). Samples were processed on a BD-Fortessa X20 or BD-LSRII flow cytometer and analyzed using FlowJo version 10 (FlowJo, LLC). Fold increases were determined by the following calculation: mean cell number at 7 dpi/ mean cell number at 4 dpi.

Preparation of recombinant CHIKV p62-E1

CHIKV p62-E1 (E3-E2-E1: residues S1-R64 of E3, S1-E161 of E2, and Y1-Q411 of E1 including a $(GGGS)_4$ polylinker between E2 and E1) of the CHIKV-LR strain was cloned into the mammalian expression vector pFM1.2 (55) with a C-terminal octa-histidine tag. The resulting plasmid was transiently expressed in FreeStyle 293-F cells using 293fectin reagent (Thermo Fisher Scientific). Cell supernatants were harvested (72 h and 120 h after transfection) and soluble CHKV p62-E1 protein captured on nickel agarose beads (Goldbio) pre-equilibrated in 50 mM Na_2HPO_4/NaH_2PO_4 pH 8.0, 300 mM NaCl, 0.125% NaN_3 and purified by Superdex 200 gel filtration chromatography in 20 mM HEPES pH 7.4 and 150 mM NaCl, 0.01% NaN_3 at 4 °C.

Antibody-dependent cellular phagocytosis (ADCP)

Recombinant CHIKV p62-E1 was biotinylated and conjugated to streptavidin-coated Alexa488 beads (Life Technologies). CHIKV p62-E1-coated beads were incubated with five-fold dilutions of antibodies (mAbs: 1 μg/ml to 0.0016 μg/ml) in culture medium for 2 h at 37°C. Monocytes harvested from the bone marrow of C57BL/6 mice and purified using a CD14+ enrichment kit (Stem Cell Technologies) were added at a concentration of 2.5×10^4 cells/well and incubated for 4 h at 37°C in low adherence 96-well plates. Following incubation, monocytes were incubated with the following antibodies: CD11b APC (BioLegend clone M1/70), CD11c AlexaFluor700 (BioLegend clone N418), and Ly6G BV421 (BioLegend clone 1A8). Cells were fixed with 4% PFA and analyzed by flow cytometry on a BD LSRII using Diva and FlowJo analysis software. The phagocytic score was determined using the following calculation: (% of AlexaFluor488$^+$ cells) x

(AlexaFluor488 geometric mean fluorescent intensity (MFI) of AlexaFluor488$^+$ cells)/ 10,000.

Antibody-dependent neutrophil phagocytosis (ADNP)

Recombinant CHIKV p62-E1 was biotinylated and conjugated to streptavidin-coated Alexa488 beads. CHIKV p62-E1-coated beads were incubated with five-fold dilutions of antibodies (mAbs: 1 μg/ml to 0.0016 μg/ml) in culture medium for 2 h at 37°C. Bone marrow cells were harvested from C57BL/6 mice. Cells were washed with PBS, and 5.0 × 10^4 cells/well were added to bead-antibody immune complexes, and incubated for 1 hour at 37°C. Cells were stained with the following antibodies: CD11b APC (BioLegend clone M1/70), CD11c AlexaFluor700 (BioLegend clone N418), Ly6G BV421 (BioLegend clone 1A8). Cells were fixed with 4% PFA and were analyzed on a BD LSRII flow cytometer. A phagocytic score was determined as described above.

Antibody depletion of immune cell subsets

For NK cell depletion, anti-NK1.1 (BioXCell clone PK136; 200 μg) or an isotype control (BioXCell clone C1.18.4; 200 μg) was administered to mice by intraperitoneal injection one day prior to and 3 dpi. For monocyte and neutrophil depletion, anti-Ly6G/Ly6C (Gr-1; BioXCell clone RB6–8C5; 500 μg) or an isotype control (BioXCell clone LTF-2; 500 μg) was administered to mice by intraperitoneal injection one day prior to and 1, 3, and 5 dpi. For neutrophil depletion, anti-Ly6G (BioXCell clone 1A8; 250 μg) or an isotype control (BioXCell clone 2A3; 250 μg) was administered to mice by intraperitoneal injection one day prior to and 1, 3, and 5 dpi. For monocyte depletion, anti-CCR2 (clone MC-21; 25 μg) (56) or an isotype control mAb (BioXCell clone LTF-2; 25 μg) was administered to mice by intraperitoneal injection on 1, 3, and 5 dpi. Anti-CHIKV mAbs or an isotype control was administered to mice by intraperitoneal injection on 3 dpi. Foot swelling was monitored using digital calipers. Following extensive perfusion, ipsilateral ankles were collected, homogenized, and processed for CHIKV infection as described above.

For analysis of immune cell depletion, peripheral blood was collected on the day of harvest. Red blood cells were lysed with ACK lysis buffer (Gibco) and resuspended in RPMI supplemented with 10% heat inactivated FBS. For NK1.1 depletion, single cell suspensions were blocked for FcγR binding and stained with CD45 BUV395, CD3 APC-Cy7, NKp46 BV421 (BioLegend clone 29A1.4; 1:50), and fixable viability dye (e506). For Ly6G/Ly6C, Ly6G, or CCR2 depletion, single cell suspensions were blocked for FcγR binding and stained with antibodies against CD45 BUV395, CD11b PerCP-Cy5.5, Ly6C Pacific Blue, Ly6B FITC, Ly6G PE-Cy7, CD11c APC, and fixable viability dye (e506).

Statistical analysis

Statistical significance was assigned with P values < 0.05 using GraphPad Prism version 7.0 (La Jolla, CA). The specific statistical test for each data set is indicated in respective figure legends and was selected based on the number of comparison groups and variance of the data. For foot swelling analysis, significance was determined by a two-way ANOVA with Tukey's post-test (more than two groups) or Sidak's post-test (between two groups). For some virological and immune cell analysis, significance was determined by one-way

ANOVA with Tukey's post-test or student's t-test. For other viral burden experiments, as well as cytokine/chemokine analysis, if data points were of unequal variance, a Kruskal-Wallis ANOVA with Dunn's post-test or Mann-Whitney test were used, depending on the number of comparison groups.

Supplementary Material

Refer to Web version on PubMed Central for supplementary material.

Acknowledgments

Funding: This work was supported by the National Institutes of Health (NIH) grants R01 AI089591 (M.S.D.), R01 AI114816 (M.S.D.), T32 AI007172 (J.M.F.), and NIH contract HHSN272201400058C (B.J.D.).

References and Notes:

1. Robinson MC, An epidemic of virus disease in Southern Province, Tanganyika Territory, in 1952–53. I. Clinical features. Transactions of the Royal Society of Tropical Medicine and Hygiene 49, 28–32 (1955). [PubMed: 14373834]
2. Staples JE, Breiman RF, Powers AM, Chikungunya fever: an epidemiological review of a re-emerging infectious disease. Clinical infectious diseases : an official publication of the Infectious Diseases Society of America 49, 942–948 (2009). [PubMed: 19663604]
3. Petersen LR, Powers AM, Chikungunya: epidemiology. F1000Research 5, (2016).
4. Schilte C, Staikowsky F, Couderc T, Madec Y, Carpentier F, Kassab S, Albert ML, Lecuit M, Michault A, Chikungunya virus-associated long-term arthralgia: a 36-month prospective longitudinal study. PLoS neglected tropical diseases 7, e2137 (2013).
5. Borgherini G, Poubeau P, Jossaume A, Gouix A, Cotte L, Michault A, Arvin-Berod C, Paganin F, Persistent arthralgia associated with chikungunya virus: a study of 88 adult patients on reunion island. Clinical infectious diseases : an official publication of the Infectious Diseases Society of America 47, 469–475 (2008). [PubMed: 18611153]
6. Strauss JH, Strauss EG, The alphaviruses: gene expression, replication, and evolution. Microbiol Rev 58, 491–562 (1994). [PubMed: 7968923]
7. Voss JE, Vaney MC, Duquerroy S, Vonrhein C, Girard-Blanc C, Crublet E, Thompson A, Bricogne G, Rey FA, Glycoprotein organization of Chikungunya virus particles revealed by X-ray crystallography. Nature 468, 709–712 (2010). [PubMed: 21124458]
8. Sun S, Xiang Y, Akahata W, Holdaway H, Pal P, Zhang X, Diamond MS, Nabel GJ, Rossmann MG, Structural analyses at pseudo atomic resolution of Chikungunya virus and antibodies show mechanisms of neutralization. eLife 2, e00435 (2013).
9. Lescar J, Roussel A, Wien MW, Navaza J, Fuller SD, Wengler G, Wengler G, Rey FA, The Fusion glycoprotein shell of Semliki Forest virus: an icosahedral assembly primed for fusogenic activation at endosomal pH. Cell 105, 137–148 (2001). [PubMed: 11301009]
10. Smith TJ, Cheng RH, Olson NH, Peterson P, Chase E, Kuhn RJ, Baker TS, Putative receptor binding sites on alphaviruses as visualized by cryoelectron microscopy. Proceedings of the National Academy of Sciences of the United States of America 92, 10648–10652 (1995). [PubMed: 7479858]
11. Zhang R, Kim AS, Fox JM, Nair S, Basore K, Klimstra WB, Rimkunas R, Fong RH, Lin H, Poddar S, Crowe JE Jr., Doranz BJ, Fremont DH, Diamond MS, Mxra8 is a receptor for multiple arthritogenic alphaviruses. Nature 557, 570–574 (2018). [PubMed: 29769725]
12. Couderc T, Khandoudi N, Grandadam M, Visse C, Gangneux N, Bagot S, Prost JF, Lecuit M, Prophylaxis and therapy for Chikungunya virus infection. The Journal of infectious diseases 200, 516–523 (2009). [PubMed: 19572805]

13. Goo L, Dowd KA, Lin TY, Mascola JR, Graham BS, Ledgerwood JE, Pierson TC, A Virus-Like Particle Vaccine Elicits Broad Neutralizing Antibody Responses in Humans to All Chikungunya Virus Genotypes. The Journal of infectious diseases 214, 1487–1491 (2016). [PubMed: 27655868]

14. Chang LJ, Dowd KA, Mendoza FH, Saunders JG, Sitar S, Plummer SH, Yamshchikov G, Sarwar UN, Hu Z, Enama ME, Bailer RT, Koup RA, Schwartz RM, Akahata W, Nabel GJ, Mascola JR, Pierson TC, Graham BS, Ledgerwood JE, Team VRCS, Safety and tolerability of chikungunya virus-like particle vaccine in healthy adults: a phase 1 dose-escalation trial. Lancet 384, 2046–2052 (2014). [PubMed: 25132507]

15. Plante K, Wang E, Partidos CD, Weger J, Gorchakov R, Tsetsarkin K, Borland EM, Powers AM, Seymour R, Stinchcomb DT, Osorio JE, Frolov I, Weaver SC, Novel chikungunya vaccine candidate with an IRES-based attenuation and host range alteration mechanism. PLoS pathogens 7, e1002142 (2011).

16. Metz SW, Martina BE, van den Doel P, Geertsema C, Osterhaus AD, Vlak JM, Pijlman GP, Chikungunya virus-like particles are more immunogenic in a lethal AG129 mouse model compared to glycoprotein E1 or E2 subunits. Vaccine 31, 6092–6096 (2013). [PubMed: 24099875]

17. Smith Scott A., Silva Laurie A., Fox Julie M., Flyak AI, Kose N, Sapparapu G, Khomadiak S, Ashbrook Alison W., Kahle Kristen M., Fong Rachel H., Swayne S, Doranz Benjamin J., McGee Charles E., Heise Mark T, Pal P, Brien James D., Austin SK, Diamond Michael S., Dermody Terence S., Crowe James E. Jr., Isolation and Characterization of Broad and Ultrapotent Human Monoclonal Antibodies with Therapeutic Activity against Chikungunya Virus. Cell host & microbe 18, 86–95 (2015). [PubMed: 26159721]

18. Pal P, Dowd KA, Brien JD, Edeling MA, Gorlatov S, Johnson S, Lee I, Akahata W, Nabel GJ, Richter MK, Smit JM, Fremont DH, Pierson TC, Heise MT, Diamond MS, Development of a highly protective combination monoclonal antibody therapy against Chikungunya virus. PLoS pathogens 9, e1003312 (2013).

19. Fox JM, Long F, Edeling MA, Lin H, van Duijl-Richter MK, Fong RH, Kahle KM, Smit JM, Jin J, Simmons G, Doranz BJ, Crowe JE Jr., Fremont DH, Rossmann MG, Diamond MS, Broadly Neutralizing Alphavirus Antibodies Bind an Epitope on E2 and Inhibit Entry and Egress. Cell 163, 1095–1107 (2015). [PubMed: 26553503]

20. Jin J, Liss NM, Chen DH, Liao M, Fox JM, Shimak RM, Fong RH, Chafets D, Bakkour S, Keating S, Fomin ME, Muench MO, Sherman MB, Doranz BJ, Diamond MS, Simmons G, Neutralizing Monoclonal Antibodies Block Chikungunya Virus Entry and Release by Targeting an Epitope Critical to Viral Pathogenesis. Cell reports 13, 2553–2564 (2015). [PubMed: 26686638]

21. Fong RH, Banik SS, Mattia K, Barnes T, Tucker D, Liss N, Lu K, Selvarajah S, Srinivasan S, Mabila M, Miller A, Muench MO, Michault A, Rucker JB, Paes C, Simmons G, Kahle KM, Doranz BJ, Exposure of epitope residues on the outer face of the chikungunya virus envelope trimer determines antibody neutralizing efficacy. Journal of virology 88, 14364–14379 (2014). [PubMed: 25275138]

22. Masrinoul P, Puiprom O, Tanaka A, Kuwahara M, Chaichana P, Ikuta K, Ramasoota P, Okabayashi T, Monoclonal antibody targeting chikungunya virus envelope 1 protein inhibits virus release. Virology 464–465, 111–117 (2014).

23. Broeckel R, Fox JM, Haese N, Kreklywich CN, Sukulpovi-Petty S, Legasse A, Smith PP, Denton M, Corvey C, Krishnan S, Colgin LMA, Ducore RM, Lewis AD, Axthelm MK, Mandron M, Cortez P, Rothblatt J, Rao E, Focken I, Carter K, Sapparapau G, Crowe JE Jr., Diamond MS, Streblow DN, Therapeutic administration of a recombinant human monoclonal antibody reduces the severity of chikungunya virus disease in rhesus macaques. PLoS neglected tropical diseases 11, e0005637 (2017).

24. Pal P, Fox JM, Hawman DW, Huang YJ, Messaoudi I, Kreklywich C, Denton M, Legasse AW, Smith PP, Johnson S, Axthelm MK, Vanlandingham DL, Streblow DN, Higgs S, Morrison TE, Diamond MS, Chikungunya viruses that escape monoclonal antibody therapy are clinically attenuated, stable, and not purified in mosquitoes. Journal of virology 88, 8213–8226 (2014). [PubMed: 24829346]

25. Morrison TE, Oko L, Montgomery SA, Whitmore AC, Lotstein AR, Gunn BM, Elmore SA, Heise MT, A mouse model of chikungunya virus-induced musculoskeletal inflammatory disease:

evidence of arthritis, tenosynovitis, myositis, and persistence. The American journal of pathology 178, 32–40 (2011). [PubMed: 21224040]

26. Gardner J, Anraku I, Le TT, Larcher T, Major L, Roques P, Schroder WA, Higgs S, Suhrbier A, Chikungunya virus arthritis in adult wild-type mice. Journal of virology 84, 8021–8032 (2010). [PubMed: 20519386]
27. Tao MH, Morrison SL, Studies of aglycosylated chimeric mouse-human IgG. Role of carbohydrate in the structure and effector functions mediated by the human IgG constant region. Journal of immunology 143, 2595–2601 (1989).
28. Nimmerjahn F, Ravetch JV, Divergent immunoglobulin g subclass activity through selective Fc receptor binding. Science 310, 1510–1512 (2005). [PubMed: 16322460]
29. Hezareh M, Hessell AJ, Jensen RC, van de Winkel JG, Parren PW, Effector function activities of a panel of mutants of a broadly neutralizing antibody against human immunodeficiency virus type 1. Journal of virology 75, 12161–12168 (2001). [PubMed: 11711607]
30. Hawman DW, Stoermer KA, Montgomery SA, Pal P, Oko L, Diamond MS, Morrison TE, Chronic joint disease caused by persistent Chikungunya virus infection is controlled by the adaptive immune response. Journal of virology 87, 13878–13888 (2013). [PubMed: 24131709]
31. Teo TH, Lum FM, Claser C, Lulla V, Lulla A, Merits A, Renia L, Ng LF, A pathogenic role for CD4+ T cells during Chikungunya virus infection in mice. Journal of immunology 190, 259–269 (2013).
32. Haist KC, Burrack KS, Davenport BJ, Morrison TE, Inflammatory monocytes mediate control of acute alphavirus infection in mice. PLoS pathogens 13, e1006748 (2017).
33. Lu LL, Suscovich TJ, Fortune SM, Alter G, Beyond binding: antibody effector functions in infectious diseases. Nature reviews. Immunology 18, 46–61 (2018).
34. Bournazos S, DiLillo DJ, Ravetch JV, The role of Fc-FcgammaR interactions in IgG-mediated microbial neutralization. The Journal of experimental medicine 212, 1361–1369 (2015). [PubMed: 26282878]
35. Poo YS, Nakaya H, Gardner J, Larcher T, Schroder WA, Le TT, Major LD, Suhrbier A, CCR2 deficiency promotes exacerbated chronic erosive neutrophil-dominated chikungunya virus arthritis. Journal of virology 88, 6862–6872 (2014). [PubMed: 24696480]
36. Hessell AJ, Hangartner L, Hunter M, Havenith CE, Beurskens FJ, Bakker JM, Lanigan CM, Landucci G, Forthal DN, Parren PW, Marx PA, Burton DR, Fc receptor but not complement binding is important in antibody protection against HIV. Nature 449, 101–104 (2007). [PubMed: 17805298]
37. Liu Q, Fan C, Li Q, Zhou S, Huang W, Wang L, Sun C, Wang M, Wu X, Ma J, Li B, Xie L, Wang Y, Antibody-dependent-cellular-cytotoxicity-inducing antibodies significantly affect the post-exposure treatment of Ebola virus infection. Scientific reports 7, 45552 (2017). [PubMed: 28358050]
38. Vogt MR, Dowd KA, Engle M, Tesh RB, Johnson S, Pierson TC, Diamond MS, Poorly neutralizing cross-reactive antibodies against the fusion loop of West Nile virus envelope protein protect in vivo via Fcgamma receptor and complement-dependent effector mechanisms. Journal of virology 85, 11567–11580 (2011). [PubMed: 21917960]
39. Li D, He W, Liu X, Zheng S, Qi Y, Li H, Mao F, Liu J, Sun Y, Pan L, Du K, Ye K, Li W, Sui J, A potent human neutralizing antibody Fc-dependently reduces established HBV infections. eLife 6, e26738 (2017).
40. DiLillo DJ, Tan GS, Palese P, Ravetch JV, Broadly neutralizing hemagglutinin stalk-specific antibodies require FcgammaR interactions for protection against influenza virus in vivo. Nature medicine 20, 143–151 (2014).
41. Gunn BM, Yu WH, Karim MM, Brannan JM, Herbert AS, Wec AZ, Halfmann PJ, Fusco ML, Schendel SL, Gangavarapu K, Krause T, Qiu X, He S, Das J, Suscovich TJ, Lai J, Chandran K, Zeitlin L, Crowe JE Jr., Lauffenburger D, Kawaoka Y, Kobinger GP, Andersen KG, Dye JM, Saphire EO, Alter G, A Role for Fc Function in Therapeutic Monoclonal Antibody-Mediated Protection against Ebola Virus. Cell host & microbe 24, 221–233 e225 (2018). [PubMed: 30092199]

42. Bournazos S, Klein F, Pietzsch J, Seaman MS, Nussenzweig MC, Ravetch JV, Broadly neutralizing anti-HIV-1 antibodies require Fc effector functions for in vivo activity. Cell 158, 1243–1253 (2014). [PubMed: 25215485]
43. He W, Chen CJ, Mullarkey CE, Hamilton JR, Wong CK, Leon PE, Uccellini MB, Chromikova V, Henry C, Hoffman KW, Lim JK, Wilson PC, Miller MS, Krammer F, Palese P, Tan GS, Alveolar macrophages are critical for broadly-reactive antibody-mediated protection against influenza A virus in mice. Nature communications 8, 846 (2017).
44. Wust CJ, Crombie R, Brown A, Passive protection across subgroups of alphaviruses by hyperimmune non-cross-neutralizing anti-Sindbis serum. Proceedings of the Society for Experimental Biology and Medicine. Society for Experimental Biology and Medicine 184, 56–63 (1987).
45. Labadie K, Larcher T, Joubert C, Mannioui A, Delache B, Brochard P, Guigand L, Dubreil L, Lebon P, Verrier B, de Lamballerie X, Suhrbier A, Cherel Y, Le Grand R, Roques P, Chikungunya disease in nonhuman primates involves long-term viral persistence in macrophages. The Journal of clinical investigation 120, 894–906 (2010). [PubMed: 20179353]
46. Hoarau JJ, Jaffar Bandjee MC, Krejbich Trotot P, Das T, Li-Pat-Yuen G, Dassa B, Denizot M, Guichard E, Ribera A, Henni T, Tallet F, Moiton MP, Gauzere BA, Bruniquet S, Jaffar Bandjee Z, Morbidelli P, Martigny G, Jolivet M, Gay F, Grandadam M, Tolou H, Vieillard V, Debre P, Autran B, Gasque P, Persistent chronic inflammation and infection by Chikungunya arthritogenic alphavirus in spite of a robust host immune response. Journal of immunology 184, 5914–5927 (2010).
47. Poo YS, Rudd PA, Gardner J, Wilson JA, Larcher T, Colle MA, Le TT, Nakaya HI, Warrilow D, Allcock R, Bielefeldt-Ohmann H, Schroder WA, Khromykh AA, Lopez JA, Suhrbier A, Multiple immune factors are involved in controlling acute and chronic chikungunya virus infection. PLoS neglected tropical diseases 8, e3354 (2014).
48. Rulli NE, Rolph MS, Srikiatkhachorn A, Anantapreecha S, Guglielmotti A, Mahalingam S, Protection from arthritis and myositis in a mouse model of acute chikungunya virus disease by bindarit, an inhibitor of monocyte chemotactic protein-1 synthesis. The Journal of infectious diseases 204, 1026–1030 (2011). [PubMed: 21881117]
49. Chen W, Foo SS, Taylor A, Lulla A, Merits A, Hueston L, Forwood MR, Walsh NC, Sims NA, Herrero LJ, Mahalingam S, Bindarit, an inhibitor of monocyte chemotactic protein synthesis, protects against bone loss induced by chikungunya virus infection. Journal of virology 89, 581–593 (2015). [PubMed: 25339772]
50. Smith SA, de Alwis AR, Kose N, Harris E, Ibarra KD, Kahle KM, Pfaff JM, Xiang X, Doranz BJ, de Silva AM, Austin SK, Sukupolvi-Petty S, Diamond MS, Crowe JE Jr., The potent and broadly neutralizing human dengue virus-specific monoclonal antibody 1C19 reveals a unique cross-reactive epitope on the bc loop of domain II of the envelope protein. mBio 4, e00873–00813 (2013).
51. Oliphant T, Engle M, Nybakken GE, Doane C, Johnson S, Huang L, Gorlatov S, Mehlhop E, Marri A, Chung KM, Ebel GD, Kramer LD, Fremont DH, Diamond MS, Development of a humanized monoclonal antibody with therapeutic potential against West Nile virus. Nature medicine 11, 522–530 (2005).
52. Tsetsarkin K, Higgs S, McGee CE, De Lamballerie X, Charrel RN, Vanlandingham DL, Infectious clones of Chikungunya virus (La Reunion isolate) for vector competence studies. Vector borne and zoonotic diseases 6, 325–337 (2006). [PubMed: 17187566]
53. Morrison TE, Whitmore AC, Shabman RS, Lidbury BA, Mahalingam S, Heise MT, Characterization of Ross River virus tropism and virus-induced inflammation in a mouse model of viral arthritis and myositis. Journal of virology 80, 737–749 (2006). [PubMed: 16378976]
54. Nair S, Poddar S, Shimak RM, Diamond MS, Interferon regulatory factor-1 (IRF-1) protects against chikungunya virus induced immunopathology by restricting infection in muscle cells. Journal of virology, (2017).
55. Mancia F, Patel SD, Rajala MW, Scherer PE, Nemes A, Schieren I, Hendrickson WA, Shapiro L, Optimization of protein production in mammalian cells with a coexpressed fluorescent marker. Structure 12, 1355–1360 (2004). [PubMed: 15296729]

56. Mack M, Cihak J, Simonis C, Luckow B, Proudfoot AE, Plachy J, Bruhl H, Frink M, Anders HJ, Vielhauer V, Pfirstinger J, Stangassinger M, Schlondorff D, Expression and characterization of the chemokine receptors CCR2 and CCR5 in mice. Journal of immunology 166, 4697–4704 (2001

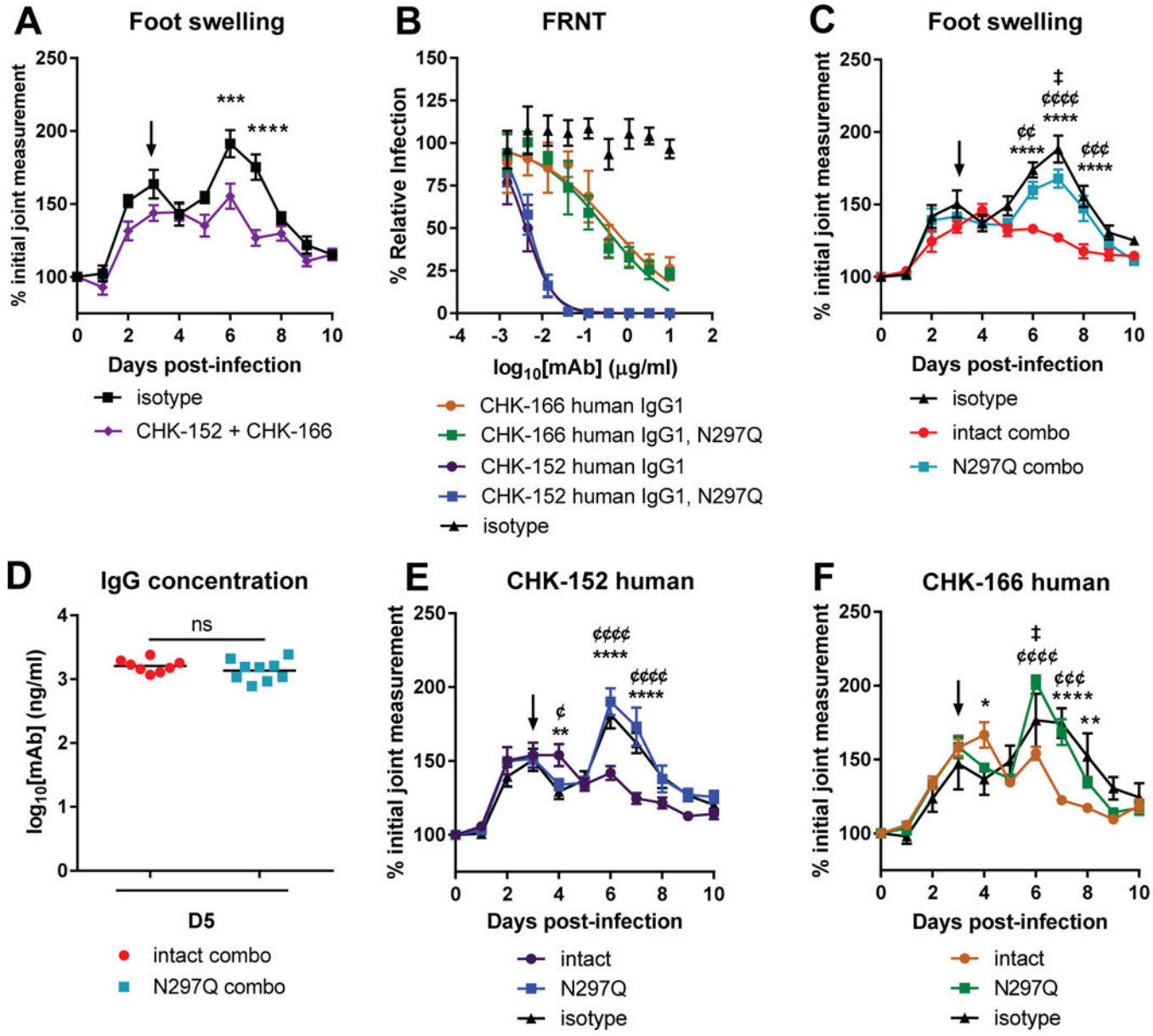

Figure 1. Clinical protection following mAb therapy.

(**A**) Four-week-old WT C57BL/6J mice were administered mouse anti-CHIKV mAbs [CHK-152 + CHK-166 (250 μg per mAb; 500 μg total)] or an isotype control (WNV E60; 500 μg) on 3 dpi with 10^3 FFU of CHIKV. Foot swelling was measured prior to infection and for 10 dpi (n = 8/group, two experiments). Graphs show means ± SEM (***, $P < 0.001$; ****, $P < 0.0001$; two-way ANOVA with Sidak's post-test). (**B**) mAbs (CHK-166 human IgG1, CHK-152 human IgG1, CHK-166 human IgG1 N297Q, CHK-152 human IgG1 N297Q) were pre-incubated with 10^2 FFU of CHIKV and added to Vero cells for 18 h. Viral foci were measured and compared to a no mAb control to determine relative infection. WNV hE16 is an isotype control mAb. Each graph represents the mean ± SD (two or three experiments). (**C-F**) Four-week-old mice were inoculated with CHIKV and then administered a (**C-D**) cocktail [CHK-152 + CHK-166 (250 μg per mAb; 500 μg total)] or

(**E-F**) monotherapy [CHK-152 or CHK-166 (250 μg total)] of intact or N297Q variants of humanized mAbs or an isotype control (WNV hE16; 500 μg or 250 μg) on 3 dpi. (**C, E, F**) Foot swelling was measured ((**C**) n = 8–10/group, three experiments; (**E**) n = 7/group, two experiments; (**F**) n = 7/group, two experiments). Graphs show means ± SEM (*intact vs isotype mAb, ¢intact vs N297Q, ‡N297Q vs isotype mAb; two-way ANOVA with Tukey's post-test, $*P < 0.05$, $**P < 0.01$, $****P < 0.0001$, $^{¢}P < 0.05$, $^{¢¢}P < 0.01$, $^{¢¢¢}P < 0.001$, $^{¢¢¢¢}P < 0.0001$, $^{‡}P < 0.05$). (**D**) Human IgG levels in the ipsilateral ankle were determined by ELISA at 5 dpi (n = 8–9/group, two experiments). Bars indicate mean values (ns, not significant; student's t-test).

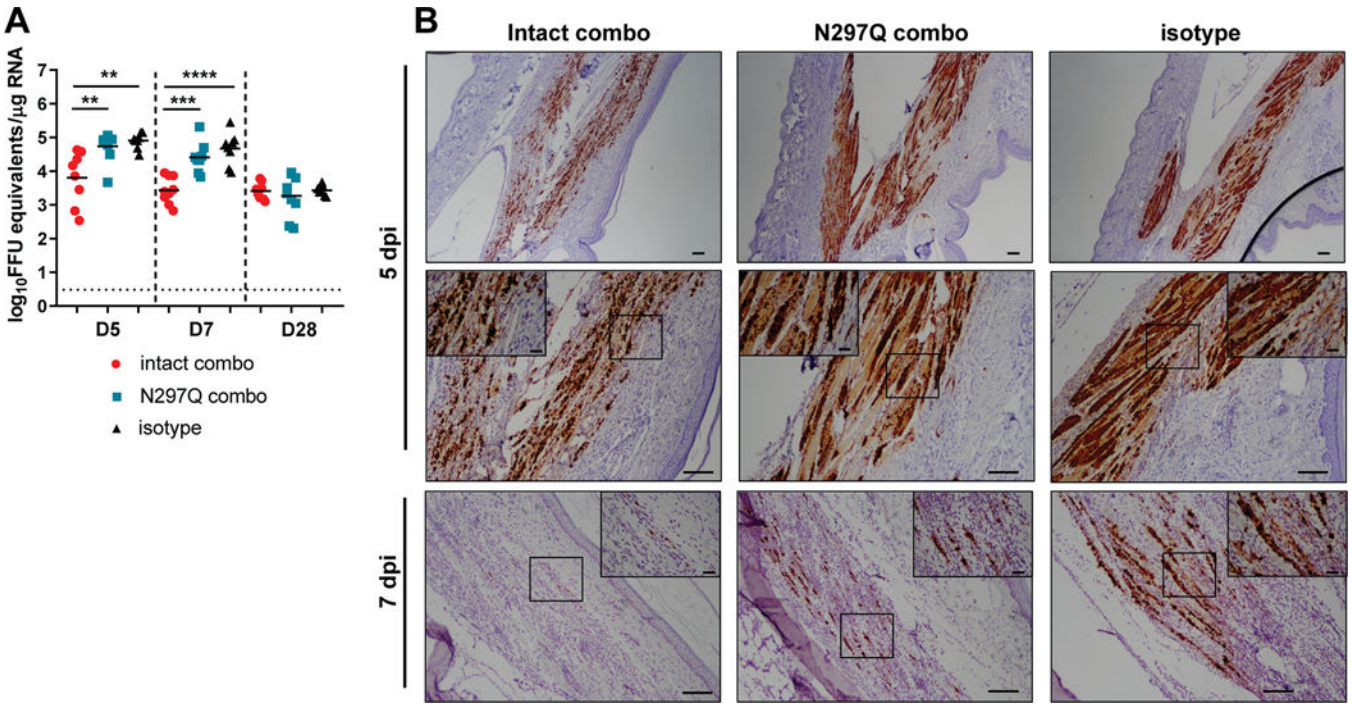

Figure 2. Intact mAb therapy reduces viral RNA levels.

WT mice were inoculated with 10^3 FFU of CHIKV and administered a cocktail of intact or N297Q variants of humanized anti-CHIKV mAbs or an isotype control mAb at 3 dpi. (**A**) Ipsilateral ankles were harvested at indicated days, and viral RNA was determined by qRT-PCR (5 and 7 dpi, n = 8–9/group, 28 dpi, n = 7–9/group, two experiments; one-way ANOVA with Tukey's post-test: *, $P < 0.05$; **, $P < 0.01$; ***, $P < 0.001$). (**B**) RNA *in situ* hybridization of ipsilateral feet using CHIKV specific probes (479501) from tissues at 5 or 7 dpi. Images show low-magnification (top; scale bar 100 μm) and medium-magnification (center and bottom; scale bar 100 μm) with a high-magnification inset (scale bar 10 μm) (representative images from n = 6/group, two experiments).

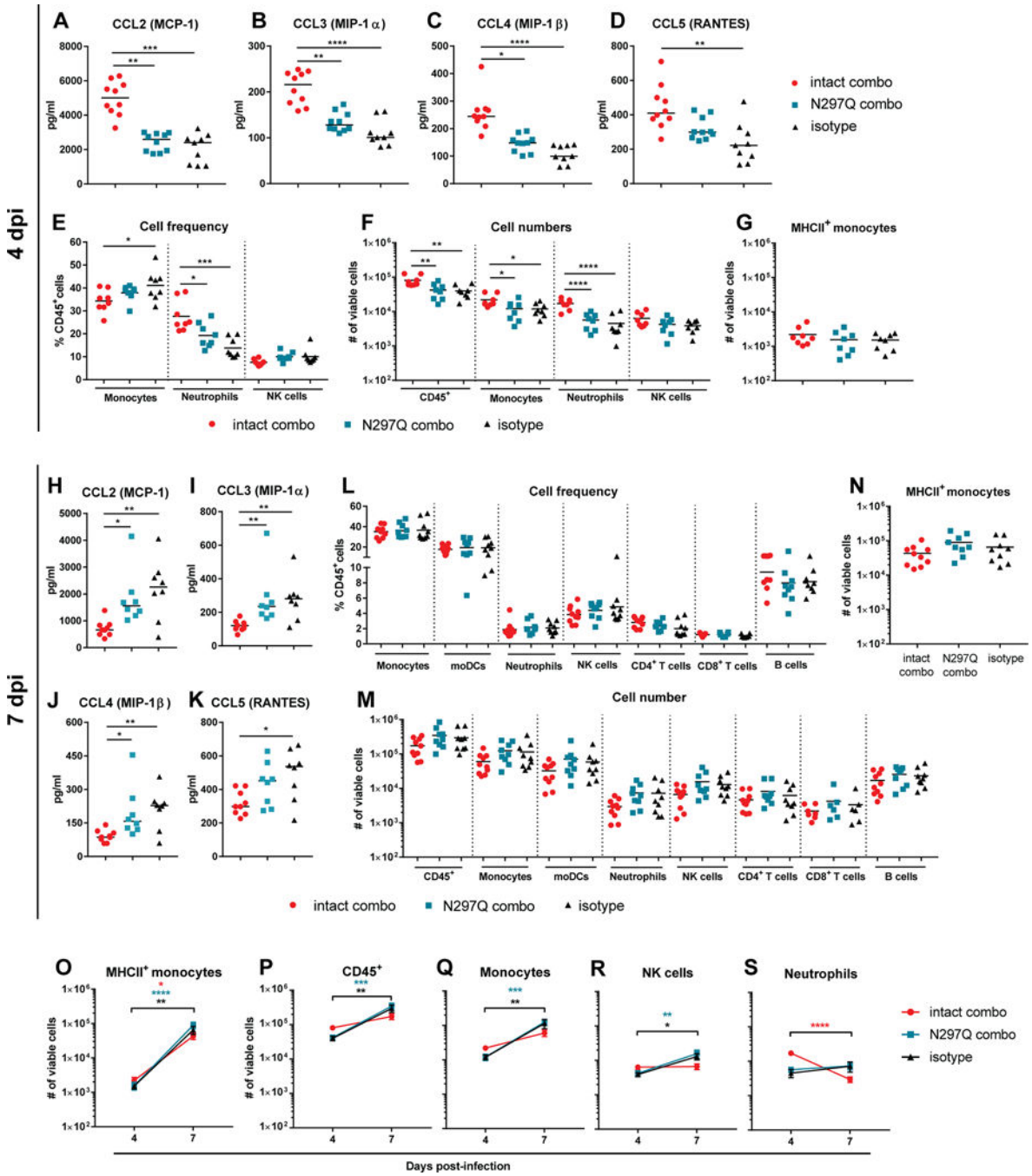

Figure 3. Fc effector functions of antibody impacts infiltration of immune cells.

WT mice were inoculated with 10^3 FFU of CHIKV and administered a cocktail of intact or N297Q variants of humanized anti-CHIKV mAbs or an isotype control at 3 dpi. (**A-D**) Ipsilateral ankles were collected at 4 dpi and analyzed for chemokines (n = 9–10/group, two experiments). Bars indicate median values (*, $P < 0.05$; **, $P < 0.01$; ***, $P < 0.001$, ****, $P < 0.0001$; Kruskal-Wallis ANOVA with Dunn's post-test). (**E-F**) At 4 dpi, cells from ipsilateral feet were stained for monocytes ($CD11b^+CD11c^-Ly6G^-Ly6C^+$), neutrophils ($CD11b^+CD11c^-Ly6G^+$), NK cells ($CD3^-NK1.1^+$), or (**G**) MHC class II^+ monocytes

($CD11b^+CD11c^-Ly6G^-Ly6C^+MHCII^+$), and analyzed by flow cytometry. (**E**) Percentage of indicated cell populations out of $CD45^+$ cells and (**F-G**) number of viable cells of indicated populations (**E-G**: n = 8/group, two experiments). Bars indicate mean values (*, $P < 0.05$; **, $P < 0.01$; ***, $P < 0.001$; one-way ANOVA with Bonferroni's post-test). (**H-K**) Ipsilateral ankles were collected at 7 dpi and analyzed for chemokines (n = 8–9/group, two experiments). Bars indicate median values (*, $P < 0.05$; **, $P < 0.01$; Kruskal-Wallis ANOVA with Dunn's post-test). (**L-M**) At 7 dpi, cells from ipsilateral feet were stained for monocytes, monocyte derived dendritic cells (moDCs) ($CD11b^+CD11c^+Ly6G^-Ly6C^+MHCII^+$), neutrophils, NK cells, $CD4^+$ T cells ($CD3^+CD4^+$), $CD8^+$ T cells ($CD3^+CD8^+$), B cells ($CD3^-CD19^+$), or (**N**) MHC class II^+ monocytes and analyzed by flow cytometry. (**L**) Percentage of indicated cell populations out of $CD45^+$ cells and (**M-N**) number of viable cells of indicated populations (**L-N**: n = 6–10/group, two or three experiments). All comparisons in **L-N** were not statistically significant (one-way ANOVA with Bonferroni's post-test). (**O-S**) Indicated cell numbers were compared between 4 and 7 dpi. Bars indicate mean ± SD (*, $P < 0.05$; **, $P < 0.01$; ***, $P < 0.001$, ****, $P < 0.0001$; student's t-test). The color of asterisks denotes significance for matching group (red, intact combo; blue, N297Q combo; black, isotype).

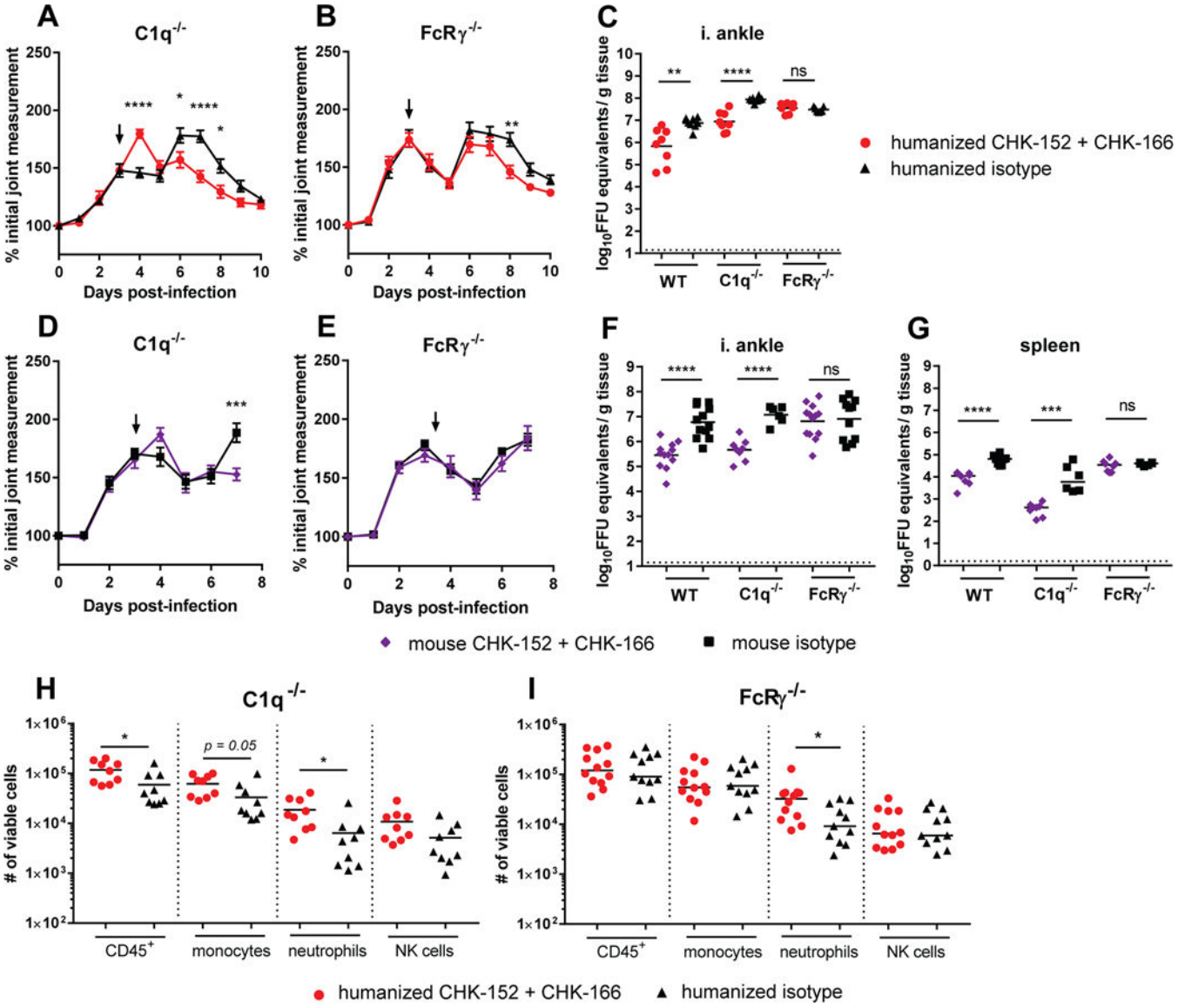

Figure 4. Fc-FcγR interactions mediate clinical and virological protection.

C1q$^{-/-}$ (**A, C-D, F-H**) or *FcRγ*$^{-/-}$ (**B-C, E-G, I**) mice were inoculated with 10^3 FFU of CHIKV and administered a cocktail of humanized (**A-C, H-I**) or mouse (**D-G**) intact anti-CHIKV mAbs or an isotype control mAb at 3 dpi. (**A-B, D-E**) Foot swelling was measured prior to infection and for 10 or 7 dpi (**A**: n = 9–10/group; **B**: n = 11–12/group; **D**: n = 6–8/group; **E**: 11–13/group, two or three experiments). Graphs show mean ± SEM (*, $P < 0.05$; **, $P < 0.01$; ***, $P < 0.001$; ****, $P < 0.0001$; two-way ANOVA with Sidak's post-test). (**C, F**) The ipsilateral ankle (i. ankle) or (**G**) spleen was harvested 5 dpi (**C**) or 7 dpi (**F-G**) and levels of viral RNA were determined. **C, F-G:** student's t-test (n = 6–13, two or three experiments; **, $P < 0.01$; ***, $P < 0.001$; ****, $P < 0.0001$; ns, not significant). (**C**) Tissue titers from WT mice are from Fig 2A (5 dpi) and shown for comparison. (**H-I**) The ipsilateral feet from antibody-treated CHIKV-inoculated *C1q*$^{-/-}$ (**H**) or *FcRγ*$^{-/-}$ (**I**) mice were harvested at 4 dpi and stained for CD45$^+$ cells, monocytes, neutrophils, NK cells, and

analyzed for number of viable cells of indicated populations by flow cytometry (**H**: n = 11–12/group, three experiments; **I**: n = 9/group, three experiments). Bars indicate mean values (*, $P < 0.05$; unpaired t test).

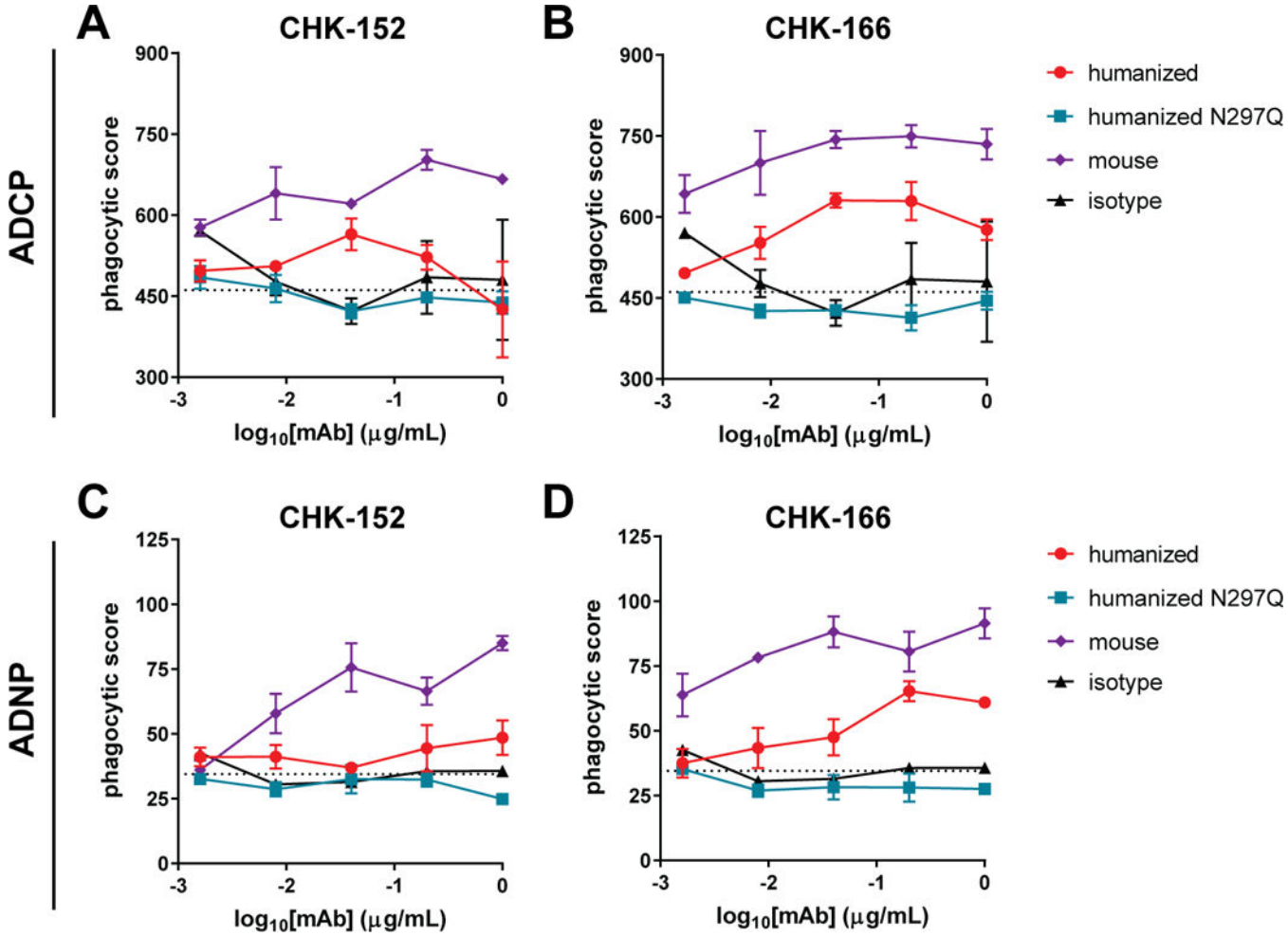

Figure 5. Anti-CHIKV mAbs enhance phagocytosis with mouse monocytes and neutrophils.

Mouse, humanized intact, and humanized N297Q variants of anti-CHIKV mAbs or an isotype control were evaluated for mouse (**A-B**) monocyte or (**C-D**) neutrophil directed phagocytosis of CHIKV p62-E1-functionalized fluorescent beads (ADCP: antibody dependent cellular phagocytosis; ADNP: antibody-dependent neutrophil phagocytosis; n = 3 donors, two experiments. The dotted line indicates the no antibody control. Graphs show mean ± SEM.

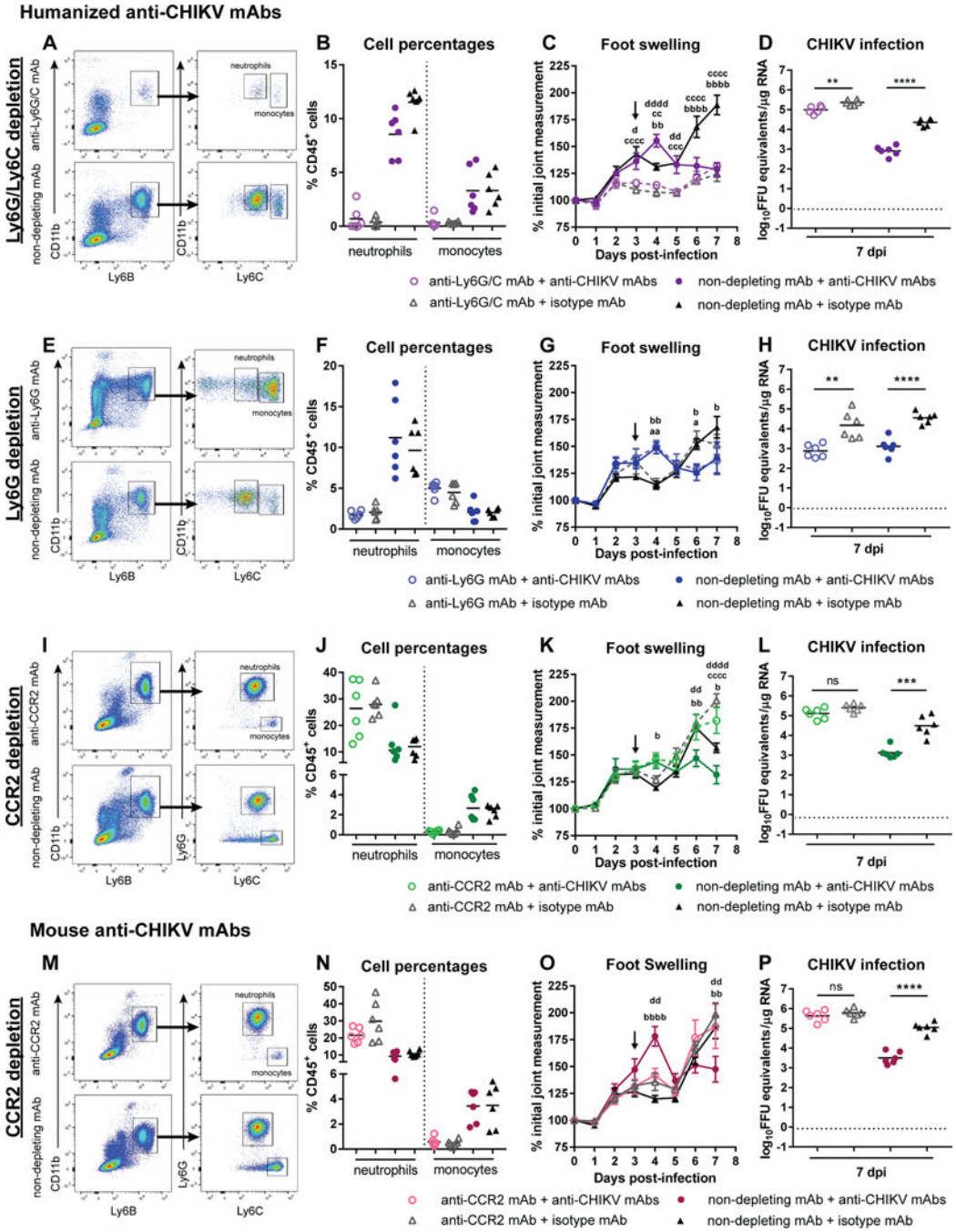

Figure 6. Monocytes reduce CHIKV infection in the context of mAb therapy.

WT mice were inoculated with 10^3 FFU of CHIKV and administered a cocktail of (**A-L**) humanized or (**M-P**) mouse intact anti-CHIKV mAbs or an isotype control mAb at 3 dpi. (**A-D**) Monocytes and neutrophils, (**E-H**) neutrophils, or (**I-P**) monocytes were depleted using anti-Ly6G/Ly6C, anti-Ly6G, or anti-CCR2, respectively. (**A-B**) Monocyte and neutrophil, (**E-F**) neutrophil, or (**I-J, M-N**) monocyte depletion was confirmed by flow cytometry analysis (**A,** anti-Ly6G/Ly6C; **E,** anti-Ly6G; or **I or M,** anti-CCR2 in each set, the top is the specific cell depletion and bottom is the non-depleting isotype). (**C, G, K, O**) Foot

swelling was measured prior to infection and for 7 dpi (**C, G, K, O**: n = 6, two experiments). Bars indicated mean ± SEM (two-way ANOVA with Tukey's post-test: **a**anti-CHIKV mAb + depleting mAb vs isotype mAb + depleting mAb (open circle vs open triangle); **b**anti-CHIKV mAb + isotype non-depleting mAb vs isotype mAb + isotype non-depleting mAb (closed circle vs closed triangle); **c**isotype mAb $^{+}$ depleting mAb vs isotype mAb + isotype non-depleting mAb (open triangle vs closed triangle); **d**anti-CHIKV mAb + depleting mAb vs anti-CHIKV mAb + isotype non-depleting mAb (open circle vs closed circle); $^{\text{a, b, or d}}$, $P < 0.05$, $^{\text{aa, bb, or dd}}$, $P < 0.01$, $^{\text{bbb or ccc}}$, $P < 0.001$, $^{\text{aaaa, bbbb, cccc, or dddd}}$, $P < 0.0001$). (**D, H, L, P**) Ipsilateral ankles were collected 7 dpi, and viral RNA levels were measured. Bars indicate mean values, and significance was determined by a student's t-test between either the depleted or isotype non-depleted ankles (**D, H, L, P**: n = 6, two experiments; **, $P < 0.01$, ***, $P < 0.001$, ****, $P < 0.0001$). Open symbols denote mice depleted of indicated immune cells, and closed symbols denote mice that receive isotype non-depleting control mAbs.